American Mineralogist, Volume 86, pages 1387–1395, 2001

Structure and elasticity of wadsleyite at high pressures

B. KIEFER,[1,]* L. STIXRUDE,[1] J. HAFNER,[2] AND G. KRESSE[2]

[1]Department of Geological Sciences, University of Michigan, Ann Arbor, Michigan 48109-1063, U.S.A.
[2]Institut für Materialphysik, Universität Wien, A-1090 Vienna, Austria

ABSTRACT

The athermal equilibrium structure, the equation of state, the elastic constants, and O atom charges were calculated for Mg_2SiO_4 wadsleyite over a range of pressures using a plane-wave pseudopotential method. The zero-pressure volume is 2% lower and the bulk modulus is 4.5% higher than experimentally observed. After correcting for zero point motion and the 300 K temperature difference between theory and experiment, using a Debye model, the calculated zero pressure volume is within 1% of experiment and the bulk modulus agrees within experimental error. The structure compresses anisotropically with linear moduli for the **a**, **b**, and **c** axes of 610 GPa, 599 GPa, and 454 GPa, respectively. The compression is largely taken up by the Mg octahedra M1, M2, and M3 which are much softer than the Si tetrahedra, with polyhedral bulk moduli of 161 GPa, 159 GPa, 157 GPa, and 331 GPa, respectively. The M1 and M3 octahedra were found to compress anisotropically which explains the greater compressibility of the **c** axis. The geometry of the Si_2O_7 group is characterized by a small Si-O-Si angle of 121.2°; compression of this group is largely accommodated by shortening of the Si-O bonds, while the inter-tetrahedral angle is almost pressure independent. We find that our results at ambient pressure are consistent with previously established systematics relating bulk modulus to volume, and Si-O-Si angle to Si-O bond length. However the variation of these quantities upon the application of pressure leads to trends that are distinct from the systematics. The calculated zero pressure elastic constants agree to within 10% with available Brillouin scattering data, with the exception of C_{12} which is 15% higher than experimentally observed. The calculated isotropically averaged bulk and shear modulus and their pressure derivatives are $K_0 = 182$ GPa, $K_0' = 4.23$, and $G_0 = 116$ GPa, $G_0' = 1.10$, respectively. The aggregate velocities and their pressure derivatives are $V_P = 9.75$ km/s, $V_P' = 0.056$ km/s/GPa, and $V_S = 5.72$ km/s, $V_S = 0.012$ km/s/GPa. We find that the elastic anisotropy of wadsleyite is intermediate between the two other Mg_2SiO_4 polymorphs, forsterite, and ringwoodite. The anisotropy is only weakly pressure dependent and decreases with increasing pressure. The azimuthal and polarization anisotropy for S waves 14.5% and 12.8% respectively, is almost pressure independent, while the azimuthal anisotropy for P waves decreases from 12.5% at ambient pressure to 10.5% in the upper part of the transition zone (14–17 GPa). Our calculated O atom charges suggest that O1 is the most likely hydroxyl site and remains so throughout the stability field of wadsleyite.

INTRODUCTION

The elasticity of wadsleyite, the intermediate pressure polymorph in the Mg_2SiO_4 system, is of considerable geophysical interest, as wadsleyite is thought to be the major mineral in the upper part of the earth's transition zone (410–520 km depth; Ita and Stixrude 1992). It is therefore expected that its elastic properties will significantly influence the seismic properties of this region (Ita and Stixrude 1992) and play an important role in our understanding of mantle composition.

Independent constraints for the composition of this region are given by the P and S wave velocities as well as the seismically observed anisotropy. To incorporate these constraints in compositional models of the upper part of the transition zone, it is necessary to know the elastic constants and their pressure dependence in the stability field of wadsleyite. The wave velocities have been determined to a pressure of 10.2 GPa from ultrasonic measurements (Li et al. 1996; Li et al. 1998), by Brillouin scattering at ambient conditions (Sawamoto et al. 1984) and to 14.2 GPa (Zha et al. 1997), just below the stability field of wadsleyite in the earth's mantle.

Wadsleyite has been proposed as a major repository for H in the upper part of the transition zone (Smyth 1987). Subsequent experiments have been performed to determine the amount of H that can be accommodated in wadsleyite (McMillan et al. 1991; Kohlstedt et al. 1996) and the most likely protonation sites (Smyth 1987; Downs 1989; Young et al. 1993; Kudoh et al. 1996). While there is general agreement that wadsleyite can incorporate significant amounts of H (up to ~3.3 wt%, Smyth 1987), it is less well resolved which of the four O atom sites are protonated. It has been proposed that only O1 is protonated (Smyth 1987), and that O1 is the most likely protonation site with additional hydrogen bonds forming to O2 (Downs 1989).

Systematics have often been invoked to provide insights into the nature of bonding in minerals. An example is the lin-

---

* E-mail: bkiefer@umich.edu

0003-004X/01/1112–1387$05.00

ear relationship between polyhedral compressibility and bond length formed at ambient conditions for a wide range of oxides and silicates (Hazen and Finger 1979). Two questions arise: (1) Do systematics apply at high pressure? (2) Is the effect of pressure similar to that of variations in composition? To investigate these two issues we look at two systematics: (1) The relationship between polyhedral compressibility and volume (Hazen and Finger 1979). (2) The relationship between the intertetrahedral angle and the bond lengths of the Si_2O_7 group. Systematics at ambient conditions show that Si-O-Si angles and Si-O bond lengths are anti-correlated (O'Keeffe and Hyde 1977; Hill and Gibbs 1979). The majority of silicates considered in these studies are characterized by Si-O-Si $\geq 130°$ and the systematics become less well constrained for small intertetrahedral angles, characteristic of wadsleyite. Therefore wadsleyite allows to investigate if the systematics apply at small Si-O-Si angles.

To address these issues we have determined the equilibrium structure, the equation of state and the elastic constants of wadsleyite up to 35 GPa which encompasses the stability field of this phase. The structural changes of wadsleyite under compression allow us to investigate the origin of the anisotropic compression and to test bulk modulus-volume systematics as well as Si-O-Si bond angle and Si-O bond length systematics. From the elastic constants we determine the aggregate wave velocities and compare them to values obtained from experiments at lower pressure. Finally we determine O atom charges to address the question of the most likely hydroxyl sites in wadsleyite.

COMPUTATIONAL METHODS

The method is based on density functional theory (DFT) and symmetry preserving, variable cell-shape structure relaxation (Wentzcovitch et al. 1993). This approach has been applied successfully to the study of structural and elastic properties of earth materials (da Silva et al. 1997; Karki et al. 1997). Computations were performed with VASP (Kresse and Hafner 1993; Kresse and Furthmüller 1996a; Kresse and Furthmüller 1996b). Two approximations were made: (1) The local density approximation (LDA) was used to describe the exchange correlation potential (parameterization of Ceperley and Alder 1980). (2) The method uses ultrasoft pseudopotentials (Vanderbilt 1990) for Mg, Si and O with $R_c = 2.000$ Bohr, $R_c = 1.800$ Bohr, and $R_c = 1.550$ Bohr for the core radii of the local potential, respectively. A conjugate gradient scheme allows for an efficient minimization of all internal structural parameters and cell shape at constant volume.

Wadsleyite crystallizes in space group *Imma* (Horiuchi and Sawamoto 1981) and contains four Mg_2SiO_4 units in the primitive cell. The structure possesses 16 degrees of freedom in the primitive unit cell (three for the cell shape and 13 internal coordinates). All calculations presented in this study were performed for the primitive unit cell. Convergence tests for wadsleyite showed that fully converged solutions to the Kohn-Sham equations can be obtained with $E_{cut} = 600$ eV and a $2 \times 2 \times 2$ Monkhorst-Pack grid (Monkhorst and Pack 1976). These computational parameters were adopted for all calculations presented here and lead to total energies that converge to within 0.3 meV/atom and Pulay stresses (Froyen and Cohen 1986) that are less than 0.03 GPa.

To address the issue of hydroxylation in wadsleyite we examined the charge of the oxygen ions. To determine the ionic charge, we integrated the self-consistent charge density within a sphere centered on the O atom site. The choice of the sphere radius is non-unique. Hence we examined the O atom charge for a range of O atom radii.

To determine the nine independent elastic constants for orthorhombic wadsleyite the equilibrium cell shape was strained by one triclinic and three orthorhombic strains (stretch along [111]). Due to the coupling between strain and lattice vibrations the structure was relaxed in the strained configuration. To obtain accurate stresses in the limit of zero strain we applied small positive and negative strains of magnitude 1%. The same methodology has been applied successfully to obtain elastic constants for other silicates (da Silva et al. 1997; Kiefer et al. 1997).

Our calculations are static, that is, they neglect zero point motion and the energetics of lattice vibrations. To correct for these effects when comparing with experimental data we have used an approximate model. The thermal pressure was calculated from a Mie-Grueneisen equation of state:

$$P_{th} = \frac{\gamma}{V}\left[E_{zpm}(V) + E_{th}(T,V)\right] \qquad (1)$$

where γ is the Grueneisen parameter, and V is the volume. The energy due to zero point motion, E_{zpm}, and the thermal energy, E_{th}, have been obtained from a Debye model:

$$E_{zpm} = \frac{9}{8}nR\theta \qquad (2)$$

and

$$E_{th}(T,V) = 9n\mathrm{R}T(T/\theta)^3\int_0^{\theta/\mathrm{T}} x^2/[\exp(x) - 1]\mathrm{d}x \qquad (3)$$

where n is the number atoms in the formula unit, T is the temperature, R is the gas constant and θ is the Debye temperature. The volume dependence of the Debye temperature and the Grueneisen parameter were described by

$$\gamma = -\frac{\partial \ln(\gamma)}{\partial \ln(V)} \qquad (4)$$

and

$$\mathrm{q} = \frac{\partial \ln(\gamma)}{\partial \ln(V)} \qquad (5)$$

where q is a constant.

RESULTS

Structure and equation of state

The calculated athermal equation of state yields a zero pressure volume that is 2% smaller than measured at ambient conditions and a bulk modulus that is 4.5% larger (Fig. 1 and Table 1). In order to compare our results directly with room temperature experimental data we estimated the thermal contributions to the equation of state. The thermal model requires three parameters: the Debye temperature, the Grueneisen parameter and the volume dependence of the Grueneisen parameter. We adopted the experimentally measured Debye temperature and Grueneisen parameter, 975 K and 1.32, respectively (Watanabe 1982). The volume dependence of the Grueneisen parameter has not been measured for wadsleyite and was assumed to be given by q = 1. After correcting for the thermal effects, the equation is in excellent agreement with experimental data, the zero pressure volume is 0.6% smaller than measured and the bulk modulus is within the experimental uncertainties. It is instructive to decompose the thermal pressure into its different contributions. For wadsleyite, a material with a high Debye temperature, approximately 80% of the thermal pressure is contributed by zero point motion, and only approximately 20% by the thermal energy at ambient temperature.

The compressional behavior of the three independent cell-edges is distinct in wadsleyite (Fig. 2). The **a** and the **b** axis are comparable in stiffness and significantly less compressible than the **c** axis. An eulerian finite strain analysis (Davies 1974) gives linear moduli K_a = 610 GPa, K_b = 599 GPa, and K_c = 454 GPa for **a**, **b**, and **c** axis, respectively. The bulk modulus calculated from these values $K_V = (K_a^{-1} + K_b^{-1} + K_c^{-1})^{-1}$ = 181 GPa is in agreement with the bulk modulus as obtained from the equation of state (Table 1).

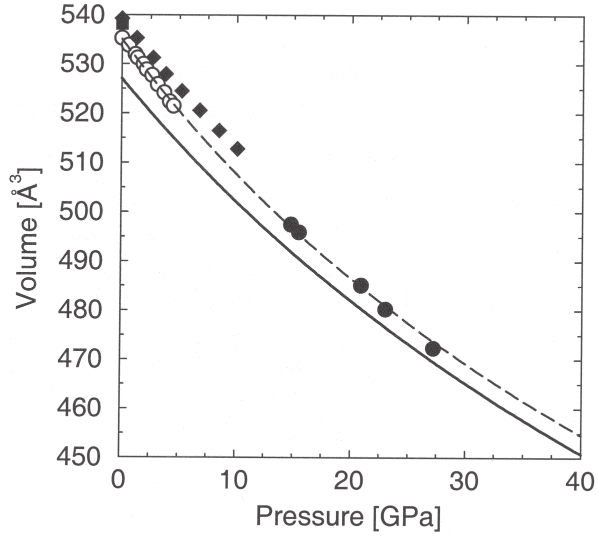

FIGURE 1. Equation of state of wadsleyite as derived from theory and experiment: Solid line = this work (0 K); dashed line = this work (300 K); filled square = Horiuchi and Sawamoto (1981); open circles = Hazen et al. (1990); open diamonds = Hazen et al. (2000); closed circles = Fei et al. (1992) after correcting volumes to $x_{Fe} = 0$ according to Jeanloz and Thompson (1983).

TABLE 1. Equation of State

V_0 (Å)	K_0 (GPa)	K_0' (–)	Reference
527.4	180.8	4.34	This study (static)
535.1	169.2	4.53	This study (300 K)
545.2	179.0	4.23	Haiber et al. (1997)*
535.30(27)	160(3)	4	Hazen et al. (1990)
539.26(4)	172(3)	6.3	Hazen et al. (2000)
538.13(7)	–	–	Horiuchi and Sawamoto (1981)

* Equation of state parameters were obtained from a Murnaghan equation of state.

Coordination polyhedra

Wadsleyite consists of Mg in octahedral and Si in tetrahedral coordination. The bulk moduli of the three symmetrically non-equivalent Mg octahedra are very similar and less than half of the bulk modulus of the Si tetrahedra (Fig. 3). The bulk moduli as obtained from a 2nd order Birch-Murnahan equation of state for the polyhedra are 161 GPa, 159 GPa, 157 GPa, and 352 GPa for M1, M2, M3, and Si polyhedra, respectively. This finding is in agreement with systematics on polyhedral bulk moduli of silicates (Fig. 1 and Hazen and Finger 1979).

The quadraticelongation and angular variance for the coordination polyhedra decrease monotonically with increasing pressure (Fig. 5a and 5b). This shows that the coordination polyhedra in wadsleyite become more regular at high pressure. The apical Mg-O bonds (parallel to the **c** axis) of the M1 and M3 sites are more compressible than the equatorial Mg-O bonds (sub-parallel to the *a,b* plane), Figure 6.

The Si_2O_7 group

Wadsleyite as a sorosilicate is characterized by Si_2O_7 groups. The Si-O bond length and the Si-O-Si angle decrease monotonically with increasing pressure (Fig. 7). However the Si-O-Si angle changes little with compression (less than 0.5°) so that the bi-tetrahedral group in wadsleyite compresses primarily by shortening of the Si-O bond. Wadsleyite has one of the smallest Si-O-Si angles observed in silicates while the bridg-

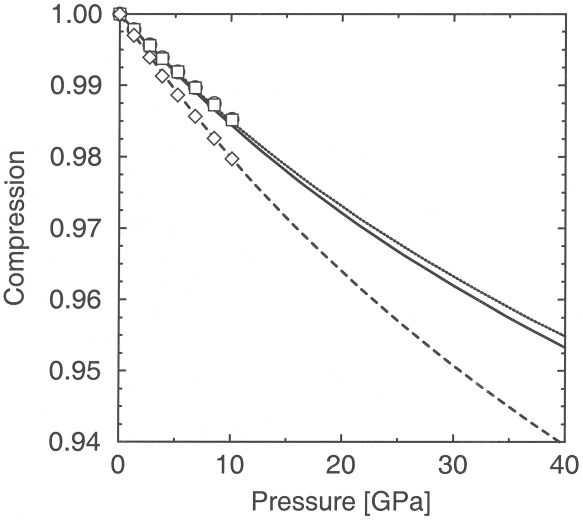

FIGURE 2. Compression of the cell edges: This work, static calculations: solid line, dotted line, and dashed line correspond to **a**, **b**, and **c** axes respectively. Experiment: open circles, open squares, and open diamonds refer to **a**, **b**, and **c** axes respectively, Hazen et al. (2000).

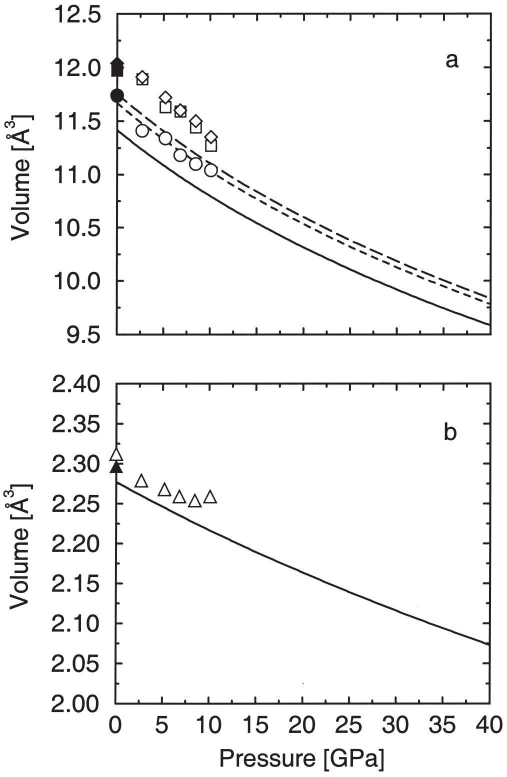

FIGURE 3. Compression of Mg octahedra and Si tetrahedra. (**a**) Compression of octahedra: solid line, dotted line, short dashed line, long-dashed line, this work for M1, M2, M3, respectively; circle, square, diamond for M1, M2, M3, respectively; closed symbols = Horiuchi and Sawamoto (1981), open symbols = Hazen et al. (2000). (**b**) Tetrahedron: solid line = this work; solid triangle = Horiuchi and Sawamoto (1981); open triangles = Hazen et al. (2000).

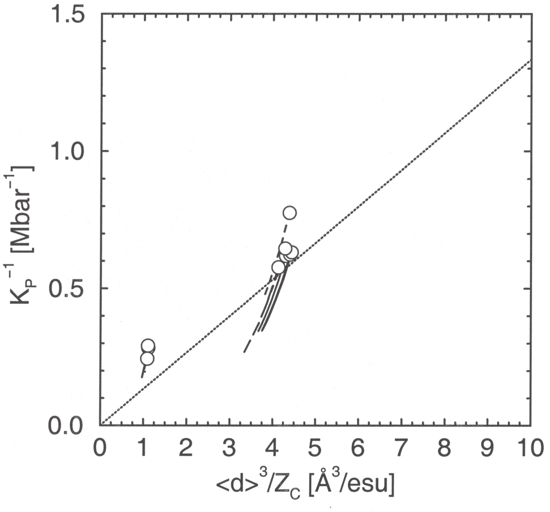

FIGURE 4. Bulk modulus-volume systematics. Wadsleyite = solid line; forsterite = short dashed line; ringwoodite = long dashed line. Systematics (Hazen and Finger 1979) = dotted line. Open circles = zero pressure values.

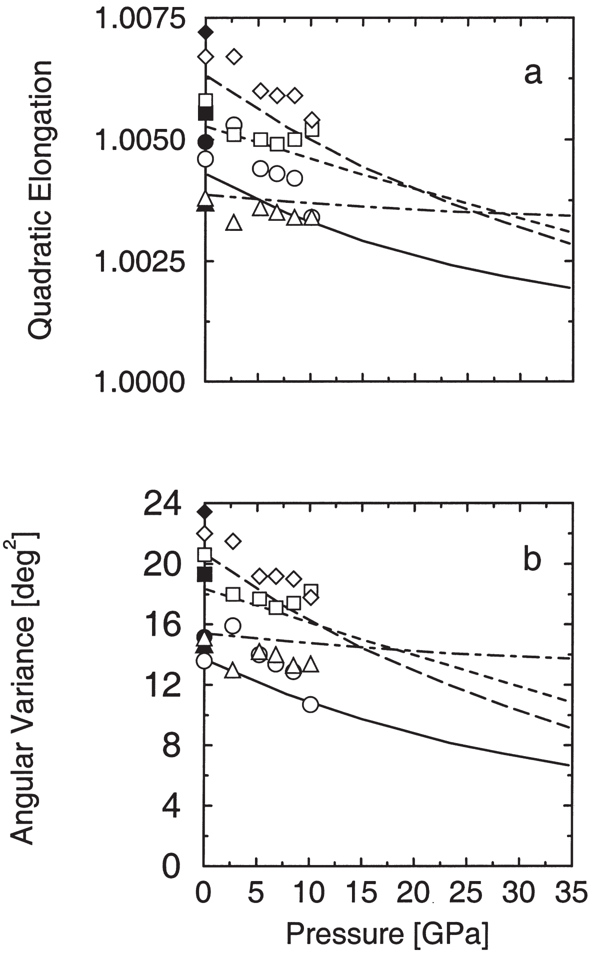

FIGURE 5. Distortion parameters for coordination polyhedra. (**a**) Quadratic elongation. (**b**) Angular variance. Symbols are the same as in Figure 3.

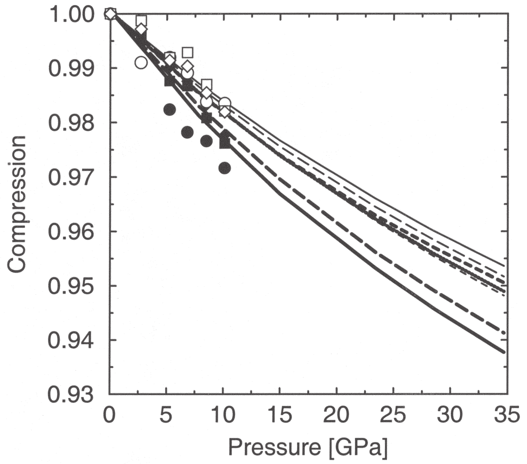

FIGURE 6. Compressibility of apical and basal dimensions of the Mg octahedra. Thick lines = apical distance; thin lines = basal distance. Solid line = dashed line, long dashed line for M1, M2, and M3, respectively. Experimental data (Hazen et al. 2000): Closed symbols = apical distances, open symbols = basal distance. Circles, squares, and diamonds for M1, M2, and M3, respectively.

ing Si-O bond is comparatively long. This finding is consistent with results from structure refinements on wadsleyite (Horiuchi and Sawamoto 1981; Hazen et al. 2000).

Elastic constants and wave velocities of wadsleyite

Our calculated athermal elastic constants agree to within 10% with experimental results (Fig. 8 and Table 2) with the exception of C_{12} which is 15% greater than experimentally observed. The relative magnitude of the calculated elastic constants is identical with experiments (Sawamoto et al. 1984; Zha et al. 1997). C_{11} and C_{22} are comparable in magnitude and significantly larger than C_{33} which is consistent with our earlier assessment that the **c** axis is more compressible than the **a** and the **b** axes. The elastic constants depend sub-linearly on pressure over the whole pressure range. However, in contrast to experiments we find a significant curvature for C_{44}, C_{55}, and C_{66} (Fig. 8b and Table 2) a behavior that has been observed in theoretical studies of forsterite (da Silva et al. 1997) and

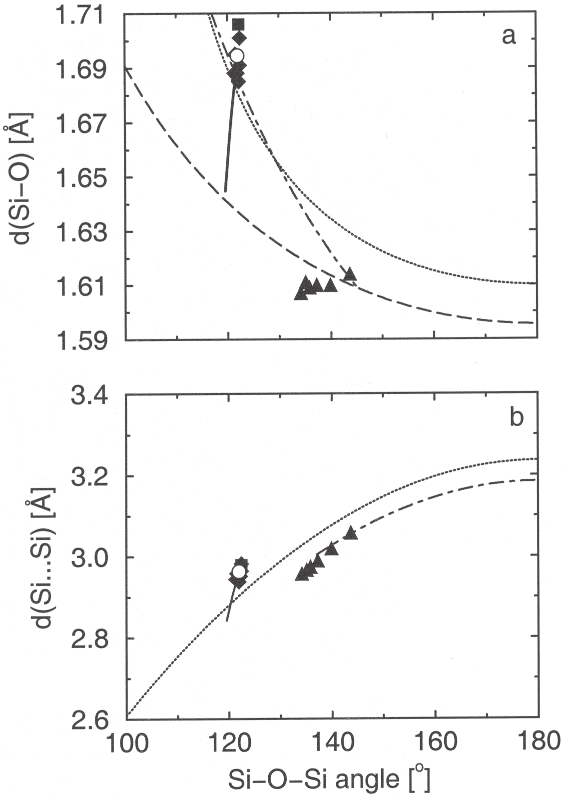

FIGURE 7. Systematics of the Si_2O_7 group. (**a**) Si-O-Si correlation to the bridging Si-O bond length. Wadsleyite: solid line = this work; open circle = this work zero pressure; filled square = Horiuchi and Sawamoto (1981); filled diamonds = Hazen et al. (2000). Coesite: filled triangles = Levien et al. (1980)}. Systematics: Short dashed line = O'Keeffe and Hyde (1977); dotted line = Hill and Gibbs (1979). Quantum-chemical calculation, long dashed line = Boisen et al. (1990). (**b**) Si-O-Si angle correlation to the Si···Si distance. Symbols are the same as in **a**, the dot dashed line is the systematics as obtained for SiO_2 polymorphs only, Hill and Gibbs (1978).

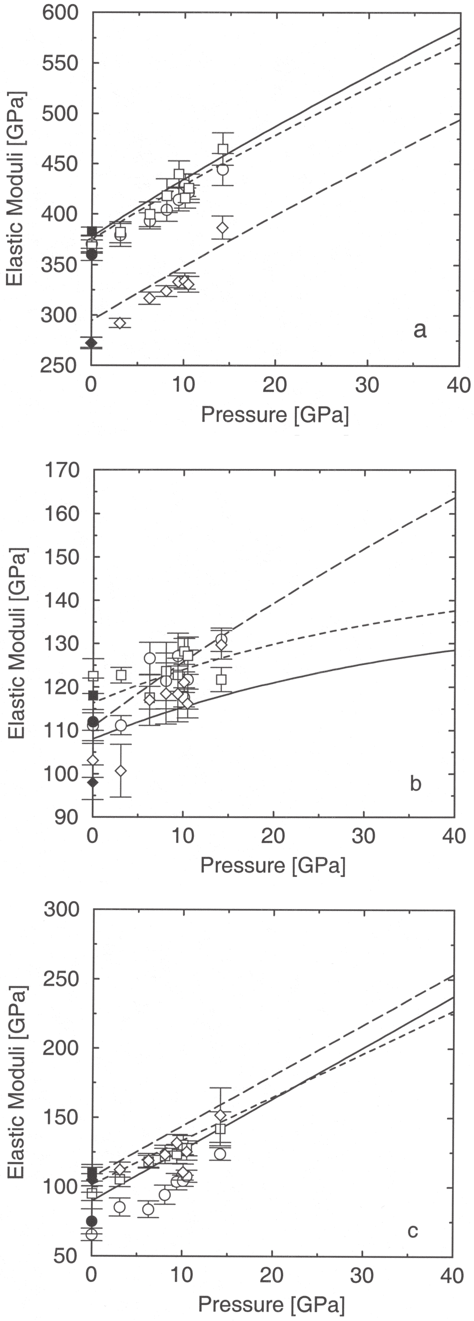

FIGURE 8. Elastic constants. Open symbols: Zha et al. (1997). Solid symbols = Sawamoto et al. (1984). (**a**) Solid line, short dashed line, and long dashed line, this work; circles, squares, diamonds, experiment for C_{11}, C_{22}, and C_{33} respectively. (**b**) Solid line, short dashed line, and long dashed line, this work; circles, squares, diamonds, experiment for C_{44}, C_{55}, and C_{66} respectively. (**c**) Solid line, short dashed line, and long dashed line, this work; circles, squares, diamonds, experiment for C_{12}, C_{13}, and C_{23} respectively.

TABLE 2. Individual elastic moduli, M_0, and their pressure derivatives M'_0 at zero pressure

	Theory		Experiment	
	M_0 (GPa)	M'_0	M_0 (GPa)*	M_0 (GPa)†
C_{11}	377	6.06	360(6)	370.5(7.8)
C_{22}	375	5.76	383(4)	367.7(6.5)
C_{33}	294	5.66	273(5)	272.4(5.8)
C_{44}	108	0.85	112(2)	111.2(3.6)
C_{55}	117	0.75	118(4)	122.5(4.0)
C_{66}	109	2.03	98(4)	103.1(3.9)
C_{12}	90	3.75	75(9)	65.6(4.5)
C_{13}	102	3.27	110(6)	95.2(5.2)
C_{23}	107	3.76	105(9)	105.1(4.4)

* Brillouin scattering data from Sawamoto et al. (1984).
† Brillouin scattering data from Zha et al. (1997). Theoretical values are from third-order finite strain fits to the first principle results.

ringwoodite (Kiefer et al. 1997). The pressure dependence of the elastic constants was represented by a third order expansion in the Eulerian finite strain (Davies 1974). We calculated Voigt-Reuss-Hill bulk- and shear-moduli and single crystal velocities of the compressional (P) and shear (S) waves to compare our results (Fig. 9 and Table 3) directly to experimental results from Brillouin scattering (Sawamoto et al. 1984; Zha et al. 1997) and ultrasonic measurements (Li et al. 1996; Li et al. 1998). The velocities as determined from our athermal elastic constants are larger than those of room-temperature experiments. Differences of this magnitude are expected due to the 300 K temperature difference between our static calculations and experiments. The pressure derivatives of the aggregate moduli and aggregate wave velocities are in good agreement with Brillouin scattering experiments (Fig. 9 and Table 3). In order to examine the pressure dependence of the seismic anisotropy and dispersion in wadsleyite, we calculated the directional dependence of the P and S wave velocity by solving the Christoffel equation. The directions of the extremal P and S wave velocities are reproduced and the calculated dispersion compare favorably with available experimental data (Fig. 10). P wave velocities are extremal for propagation along [100] and [001]. The greatest shear wave velocity is in the [110] propagation direction throughout the whole pressure range. The least shear wave velocity at low pressures is in the $[1/2,1/2,1/\sqrt{2}]$ propagation direction while at high pressures it is in the [001] direction.

To investigate the elastic anisotropy in wadsleyite we consider three measures:

$$\Delta_{\mathrm{S,polarization}} = \frac{\max\left[V_{\mathrm{S1}}(\vec{n}) - V_{\mathrm{S2}}(\vec{n})\right]}{V_{\mathrm{S,aggregate}}} \tag{6}$$

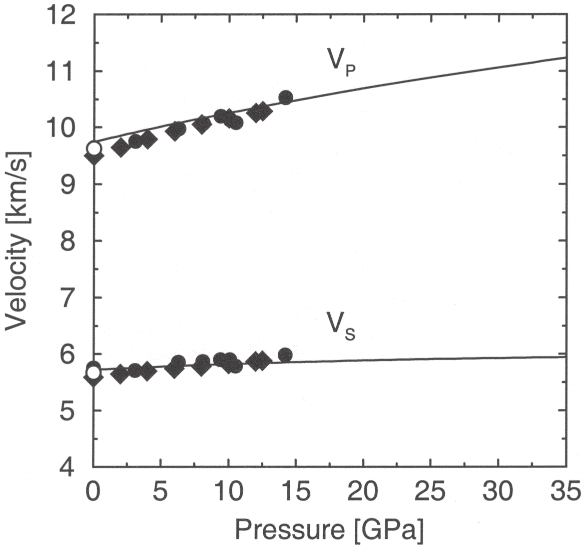

FIGURE 9. Voigt-Reuss-Hill averages of the compressional and shear-velocity: solid lines = this work; open circles = Sawamoto et al. (1984); filled circles = Zha et al. (1997); filled diamonds = Li et al. (1998).

$$\Delta_{\mathrm{S,azimuthal}} = \frac{\max\left[V_{\mathrm{S}}(\vec{n})\right] - \min[V_{\mathrm{S}}(\vec{n})]}{V_{\mathrm{S,aggregate}}} \tag{7}$$

$$\Delta_{\mathrm{P,azimuthal}} = \frac{\max\left[V_{\mathrm{P}}(\vec{n})\right] - \min[V_{\mathrm{P}}(\vec{n})]}{V_{\mathrm{P,aggregate}}} \tag{8}$$

where $\vec{n}$ is the propagation direction. Evaluating these expressions from the dispersion relations show that the anisotropy depends only weakly on pressure (Fig. 11). The magnitude $\Delta_{\mathrm{S,polarization}}$, $\Delta_{\mathrm{S,azimuthal}}$, and $\Delta_{\mathrm{P,azimuthal}}$ of wadsleyite is intermediate between olivine (da Silva et al. 1997) and ringwoodite (Kiefer et al. 1997). The predicted anisotropies are smaller than experimentally measured. This is a consequence of the systematic differences of the dispersion relation in the extremal velocity directions (Fig. 10).

OH in Wadsleyite

Wadsleyite has been considered as a prime candidate for hydrogen storage in the upper part of the transition zone. According to Pauli bond strength arguments (Smyth 1987, Table 4) O1 is the most likely hydroxyl site. O2, the bridging O atom of the Si_2O_7 group has been suggested as a hydroxyl site (Downs 1989) in addition to O1. To determine the most likely protonation site we integrated the equilibrium charge density surround-

TABLE 3. Aggregate elastic properties and pressure derivatives (in parenthesis)

K (GPa),[–]	G (GPa),(–)	V_P (km/s),(km/s GPa)	V_S (km/s),(km/s GPa)	Reference
182(4.23)	116(1.10)	9.75(0.056)	5.72(0.012)	This study (static)
174(–)	114(–)	9.66(–)	5.71(–)	Sawamoto et al. (1984)
174(4.3)	115(1.4)	9.66(0.064)	5.71(0.019)	Zha et al. (1997)
170(4.5)	108(1.6)	9.51(0.073)	5.60(0.025)	Li et al. (1996)
172(4.2)	113(1.5)	9.63(0.065)	5.67(0.021)	Li et al. (1998)

Note: The theoretical moduli are Voigt-Reuss-Hill averages, calculated from the elastic constants. The values of K_0 and K'_0 are consistent with the values derived from the equation of state (Table 1). Experimental values are Voigt-Reuss-Hill averages. Values in parentheses refer to pressure derivatives.

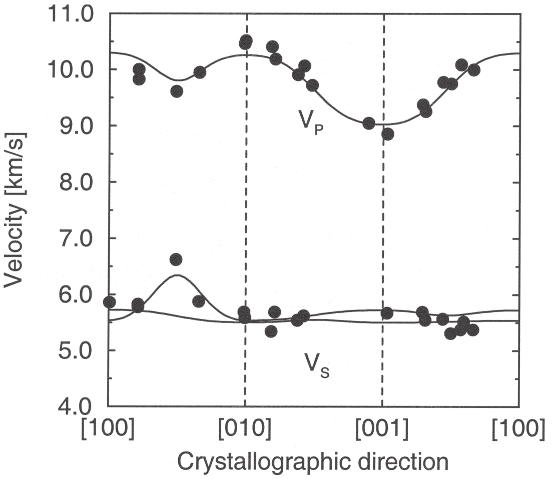

FIGURE 10. Elastic wave velocities as a function of propagation direction. This work = solid lines; Experimental data: solid circles = Sawamoto et al. (1984).

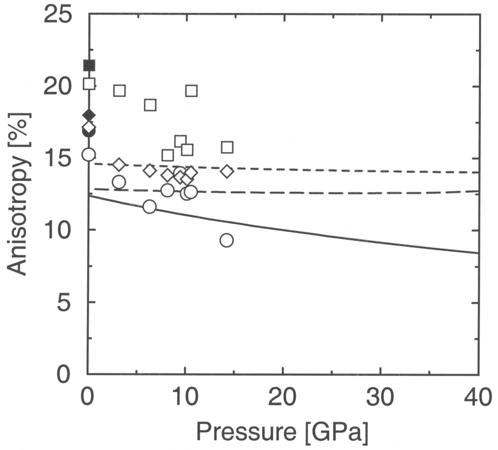

FIGURE 11. Single-crystal anisotropy. $\Delta_{P,azimuthal}$: Solid line = this work; open circles = Zha et al. (1997); solid circles = Sawamoto et al. (1984). $\Delta_{S,azimuthal}$: Short dashed line = this work; open squares = Zha et al. (1997); solid squares = Sawamoto et al. (1984). $\Delta_{S,polarization}$: Long dashed line = this work; open diamonds = Zha et al. (1997); solid diamonds = Sawamoto et al. (1984).

ing the four symmetrically non-equivalent O atom sites. However, the radii are arbitrary and therefore we examined a range of different radii (Fig. 12 and Table 4). As expected the O atom charges increase with increasing sphere radius. However, the relative magnitude of the charges on the four O atoms does not depend on the radius.

DISCUSSION

It is widely assumed that the LDA leads to an overbinding of structures and hence theoretically calculated volumes that are smaller than those experimentally observed. However, the comparison is often indirect; whereas most theoretical calculations are athermal, most experimental measurements are performed at ambient temperature. We find that after correcting for thermal effects, LDA yields essentially perfect agreement with experiment results. The agreement may be fortuitously good as other approximations may also affect the theoretical results including the pseudopotential approximation (Stixrude et al. 1998). Nevertheless, the results show that, at least in the case of wadsleyite, the incorporation of thermal effects is essential for gauging the accuracy of LDA. For materials with large Debye temperatures, such as wadsleyite, the zero-point motion is the largest vibrational contribution. The importance of properly accounting for zero-point motion when comparing theory with experiments has also been emphasized by Li and Jeanloz (1987) in the context of pressure-induced phase transformations. Thermal corrections may also be important for evaluating the performance of other approximations to the exchange correlation potential. For example, the Generalized Gradient Approximation (GGA) (Perdew et al. 1996) includes additional terms beyond the LDA that are essential for an accurate description of Fe (Bagno et al. 1989; Stixrude et al. 1994). In the case of oxides, there is some evidence that GGA predictions of energetics are superior to those of LDA (Hamann 1996). However, GGA tends to underbind oxides, that is to overestimate their volume, a tendency that would be made worse by the incorporation of thermal corrections.

Our results show in agreement with experimental results

TABLE 4. Oxygen charges

Pressure (GPa)	O1	O2	O3	O4	Reference
—	1.67	2.33	2.00	2.00	Smyth (1987)
0	1.42	1.71	1.55	1.57	This study
35	1.58	1.85	1.71	1.72	This study
0	0.57	0.94	0.79	0.78	Haiber et al. (1997)

Note: Radii for the O atoms have been fixed at $r_O = 1.54$ Å. The values from the ab-initio study by Haiber et al. (1997) were obtained from a Mullikan population analysis.

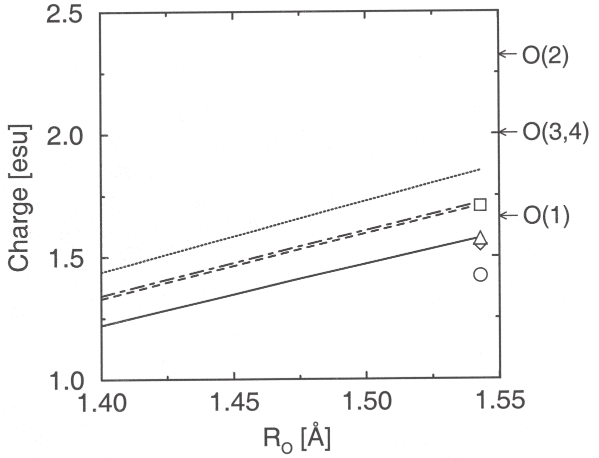

FIGURE 12. Dependence of the calculated O atom charges on sphere radii. This work (35 GPa): solid line = O1, dotted line = O2, short dashed line = O3 and dot dashed line = O4. This work (0 GPa): circle, square, diamond, and triangle represent O1, O2, O3, and O4 respectively. The values as obtained from Pauling bond strengths are indicated by the arrows (Smyth 1987).

that the **c** axis is much more compressible than the **a** and the **b** axes (Fig. 2). To analyze the origin of the compressional anisotropy, we examine the compression of individual coordination polyhedra. Most of the volume compression is taken up by the Mg octahedra; by comparison the Si tetrahedral volume, and the Si-O-Si angles change little with compression (Figs. 3 and 7). The Mg octahedra share edges sub-parallel to [100], [010], and [111]. One expects that shared edges will be stiffer than unshared edges and that the octahedra will compress anisotropically as a result. In particular, since there are no shared edges sub-parallel to [001], this direction should be more compressible. This is illustrated by comparing the compression of apical Mg-O bonds (parallel to **c**) with that of the equatorial Mg -O bonds (in the a-b plane). The apical bonds of the M1 and M3 octahedra are softer than the corresponding equatorial bonds (Fig. 6), while apical and equatorial bonds compress similarly for M2. Thus the softer **c** axis originates in the anisotropic compression of the M1 and M3 octahedra.

An assessment of the compression of the coordination polyhedra shows that the Si tetrahedron is more than twice as stiff as compared to the Mg octahedra (Fig. 3). A similar observation has been made for other silicates (Hazen and Finger 1979). Correlating the effect of pressure on different structural units allow us to provide a different view of systematics that have been proposed in the past. Systematics commonly consider the variability of structural properties with changing chemical composition. But do the same systematics apply at high pressure and is the effect of pressure analogous to that of compositional variations? A similar idea has been applied to study Birch's law at high pressures (Campbell and Heinz 1992).

Hazen and Finger (1979) found a linear relationship between polyhedral compressibility and polyhedral volume for a wide range of silicates at ambient conditions (Fig. 4). Calculating the same properties at ambient conditions in wadsleyite from our results, we find agreement with the proposed systematics. However, considering the effect of pressure, our results show a distinct trend. The trend as defined by variations in compressibility and volume upon the application of pressure is oblique, showing that pressure and variations in composition have different signatures. We have also examined the properties of Mg- and Si-polyhedra in the other two Mg_2SiO_4 polymorphs, forsterite and ringwoodite, as obtained from first principle calculations (da Silva et al. 1997; Kiefer et al. 1998) (Fig. 4). The effect of pressure is found to be similar for all Mg_2SiO_4 polymorphs.

Wadsleyite as a sorosilicate is characterized by its Si_2O_7 groups. In wadsleyite, this structural group has a very small inter-tetrahedral angle and a long bridging Si-O bond length. Compression of this group is largely accommodated by the shortening of the Si-O bond length rather than changing the Si-O-Si angle (Fig. 7a). This finding in our calculations agrees well with experiments (Horiuchi and Sawamoto 1981; Hazen et al. 2000). Our results at ambient conditions agree well with previously established systematic relationships between the Si-O-Si angle and the bridging Si-O bond length (O'Keeffe and Hyde 1977; Hill and Gibbs 1979). However, we find again that the effect of pressure produces a trend that is oblique to the systematics established at ambient conditions (Fig. 7). Experimental data for coesite (Levien et al. 1980) lend further support to this conclusion but at larger Si-O-Si angles.

We note that the relationship between Si-O-Si angle and Si-O bond length as obtained from quantum-chemical calculations for the $H_6Si_2O_7$ molecule (Gibbs 1982; Boisen et al. 1990) disagrees with our results and empirical systematics. The disagreement is particularly pronounced in the case of wadsleyite with a small Si-O-Si angle. A careful analysis of the quantum-chemical calculations (Burkhard et al. 1991) showed that the calculations may be systematically biased by the formation of O···H bonds at low Si-O-Si angles. The formation of an O-H···O bond could lead to enhanced bonding between terminating hydrogens of one tetrahedron with the closest O atom of the other tetrahedron, therefore artificially reducing the Si-O-Si angle for a given Si-O bond length.

Wadsleyite can accommodate significant amounts of water (Smyth 1987). This is expected to have a significant influence on the rheological properties of this phase and therefore the dynamics in the upper part of the transition zone and it is necessary to understand where the hydrogen resides in the structure. Smyth (1987) proposed on the basis of a Pauling bond strength analysis that O1 is the hydroxyl site. This is in general agreement with the finding of X-ray diffraction experiments (Kudoh et al. 1996). Inversion of observed X-ray amplitudes to obtain the electrostatic energy surface throughout the crystal showed that O1 and O2 are likely protonation sites (Downs 1989). Furthermore, IR measurements show at least two distinct peaks in the OH stretching region (McMillan et al. 1991). To address the question of which of the O atom sites in wadsleyite are most likely protonated we calculated charges for the crystallographically non-equivalent O atoms and obtained the following order: $q_{O1} < q_{O3} < q_{O4} < q_{O2}$ (Fig. 12 and Table 4). With this method each O atom is considered to be spherical. The integrated charge density in the sphere is considered the charge of the O atom. The radii are not determined uniquely but a study of the sensitivity of our results with respect to changes in the O atom radii shows that the order remains unaffected by changes of radii (Fig. 12). This indicates that O1 is the most likely protonation site while O2 is least likely to be protonated. This finding confirms the predictions from Pauli bond strength arguments (Smyth 1987) and semi-empirical calculations for the protonation of the O atom sites in wadsleyite (Wright and Catlow 1996) and previous ab-initio calculations (Haiber et al. 1997).

The two IR peaks in the OH-stretching region observed experimentally may indicate that the hydrogens are disordered, between O1-H···O3 and O1-H···O4 (Kudoh et al. 1996). Based on our calculated bond lengths for O1-O3 and O1-O4 and OH stretching systematics (Sikka 1997; Nakamoto 1955) we estimated OH stretching frequencies of 3550 cm^{-1} and 3220 cm^{-1} for O1-H···O3 and O1-H···O4 respectively at zero pressure. These frequencies are somewhat lower than observed experimentally, 3580 cm^{-1} and 3324 cm^{-1}. Using systematics for OH stretching frequencies we calculated that O1···O3 and O1···O4 would have to lengthen by 0.01 Å and 0.04 Å respectively to match the observed IR frequencies (McMillan et al. 1991). This may be due to the fact that protonation requires formation of defects to maintain charge neutrality. The induced relaxation around the defect may change the vibrational frequencies. A mechanism of this type has been suggested as a possible explanation for the experimentally observed hydrolytic weakening of forsterite (Brodholt and Refson 2000).

ACKNOWLEDGMENTS

This work was supported by National Science Foundation grant EAR-9973139.

REFERENCES CITED

Bagno, P., Jepsen, O., and Gunnarson, O. (1989) Ground-state properties of third-row elements with nonlocal density functionals. Physical Review B, 40, 1997–2000.

Boisen, M.B., Gibbs, G.V., Downs, R.T., and D'Arco, P. (1990) The dependence of the SiO bond length on the structural parameters in coesite, the silica polymorphs, and the clathrasils, American Mineralogist, 75, 748–756.

Brodholt, J.P. and Refson, K. (2000) An ab initio study of hydrogen in forsterite and a possible mechanism for hydrolytic weakening. Journal of Geophysical Research, 105, 18977–18982.

Burkhard, D.J., DeJong, B.H., Mayer A.J., and Van Lenthe, J.H. (1991) $H_6Si_2O_7$: Ab initio molecular orbital calculations show two geometric conformations. Geochimica and Cosmochimica Acta, 55, 3453–3458.

Campbell, A.J. and Heinz, D.L. (1992) A High-Pressure Test of Birch's Law. Science, 257, 66–68.

Ceperley, D.M. and Alder, B.J. (1980) Ground-state of the electron-gas by a stochastic method. Physical Review Letters, 45, 566–569.

da Silva, C., Stixrude, L., and Wentzcovitch, R.M. (1997) Elastic anisotropy of fosterite at high pressure. Geophysical Research Letters, 24, 1963–1966.

Davies, G.F. (1974) Effective elastic moduli under hydrostatic stress - I. quasi harmonic theory. Journal of the Physics and Chemistry of Solids, 35, 1513–1520.

Downs, J. W. (1989) Possible site for protonation in β-Mg_2SiO_4. American Mineralogist, 74, 1124–1129.

Fei, Y., Mao, H.K., Shu, J., Parthasarathy, G., Bassett, W.A., and Ko, J. (1992) Simultaneous high-*P*, high-*T* X-ray diffraction study of β-$(Mg,Fe)_2SiO_4$ to 26 GPa and 900 K. Journal of Geophysical Research, 97, 4489–4495.

Froyen, S. and Cohen. M.L. (1986) Structural properties of NaCl and KCl under pressure. Journal of Physics C: Solid State Physics, 19, 2623–2632.

Gibbs, G.V. (1982) Molecules as models for bonding in silicates, American Mineralogist, 67, 421–450.

Haiber, M., Ballone, P., and Parrinello, M. (1997) Structure and dynamics of protonated Mg_2SiO_4: An ab-initio molecular dynamics study. American Mineralogist, 97, 913–922.

Hamann, D.R. (1996) Generalized gradient theory for silica phase transitions, Physics Review Letters, 76, 660–663.

Hazen, R.M. and Finger, L.W. (1979) Bulk modulus-volume relationship for cation-anion polyhedra. Journal of Geophysical Research, 84, 6723–6728.

Hazen, R.M., Zhang, J.M., and Ko, J. (1990) Effects of Fe/Mg on the compressibility of synthetic wadsleyite: β-$(Mg_{1-x}Fe_x)_2SiO_4$ ($x \leq 0.25$). Physics and Chemistry of Minerals, 17, 416–419.

Hazen, R.M., Weinberger, M.B., Yang, H., and Prewitt, C.T. (2000) Comparative high-pressure chemistry of wadsleyite, β-$(Mg_{1-x}Fe_x)_2SiO_4$, with $x = 0$ and $x = 0.25$. American Mineralogist, 85, 770–777.

Hill, R.J. and Gibbs, G.V. (1979) Variation in d(T-O), d(T···T) and TOT in silica and silicate minerals, phosphates and aluminates. Acta Crystallographica B, 35, 25–30.

Horiuchi, H. and Sawamoto, H. (1981) β-$(Mg_{1-x}Fe_x)_2SiO_4$: Single-crystal X-ray diffraction study. American Mineralogist, 66, 568–575.

Ita, J. and Stixrude, L. (1992) Petrology, elasticity, and composition of the mantle transition zone. Journal of Geophysical Research, 97, 6849–6866.

Jeanloz, R. and Thompson, A.B. (1983) Phase transitions and mantle discontinuities. Reviews of Geophysics and Space Physics, 21(1), 51–74.

Karki, B.B., Stixrude, L., Clark, S.J., Warren, M.C., Ackland, G.J., and Crain, J. (1997) Structure and elasticity of MgO at high pressure. American Mineralogist, 82, 52–61, 1997.

O'Keeffe, M. and Hyde, B.G. (1977) On Si-O-Si configurations in silicates. Acta Crystallographica, B34, 27–32.

———(1997) Calculated elastic constants and anisotropy of Mg_2SiO_4 spinel at high pressure. Geophysical Research Letters, 24, 2841–2844.

Kiefer, B., Stixrude, L., and Wentzcovitch, R.M. (1998) Normal and inverse ringwoodite at high pressures. American Mineralogist, 84, 288–293.

Kohlstedt, D.L., Keppler, H., and Rubie, D.C. (1996) Solubility of water in the α, β, and γ phases of $(Mg,Fe)_2SiO_4$. Contributions to Mineralogy and Petrology, 123, 345–357.

Kresse, G. and Hafner, J. (1993) Ab initio molecular-dynamics for liquid-metals. Physical Review B, 47(1), 558–561.

Kresse, G. and Furthmüller, J. (1996a) Efficient iterative schemes for ab initio total-energy calculations using a plane-wave basis set. Physical Review B, 54(16), 11169–11186.

———(1996b) Efficiency of ab-initio total energy calculations for metals and semiconductors using a plane-wave basis set. Computational Materials Science, 6(1), 15–50.

Kudoh, Y., Inoue, T., and Arashi, H. (1996) Structure and crystal chemistry of hydrous wadsleyite, $Mg_{1.75}SiH_{0.5}O_4$: possible hydrous magnesian silicate in the mantle transition zone. Physics and Chemistry of Minerals, 23, 461–469.

Levien, L., Prewitt, C.T., and Weidner, D.J. (1980) Structure and elastic properties of quartz at pressure. American Mineralogist, 65, 920–930.

Li, B., Gwanmesia, G.D., and Liebermann, R.C. (1996) Sound velocities of olivine and beta polymorphs of Mg_2SiO_4 at earth's transition zone pressures. Geophysical Research Letters, 23, 2259–2262.

Li, B., Liebermann, R.C., and Weidner, D.J. (1998) Elastic moduli of wadsleyite (β-Mg_2SiO_4) to 7 gigapascals and 873 kelvin. Science, 281, 675–677.

Li, X.Y. and Jeanloz, R. (1987) Measurement of the B1-B2 transition pressure in NaCl at high-temperatures. Physical Review B, 36(1), 474–479.

McMillan, P.F., Akaogi, M., Sato, R.K., Poe, B., and Foley, J. (1991) Hydroxyl groups in β-Mg_2SiO_4. American Mineralogist, 76, 354–360.

Monkhorst, H. J. and Pack, J. D. (1976) Special points for Brillouin-zone integrations. Physical Review B, 23, 5048–5192.

Nakamoto, K., Arrgoshes, M., and Rundle, R.E. (1955) Stretching frequencies as a function of distances in hydrogen bonds. Journal of Chemical Physics, 77, 6480–6486.

Perdew, J.P., Burke, K., and Ernzerhof, M. (1996) Generalized gradient approximations made simple. Physical Review Letters, 77, 3865–3868.

Sawamoto, H., Weidner, D.J., Sasaki, S., and Kumazawa, M. (1984) Single-crystal elastic properties of the modified spinel (beta) phase of magnesium orthosilicate. Science, 224, 749–751.

Sikka, S.K. (1997) Hydrogen bonding under pressure. Indian Journal of Pure and Applied Physics, 35, 677–681.

Smyth, J.R. (1987) β-Mg_2SiO_4: A potential host for water in the mantle. American Mineralogist, 72, 1051–1055.

Stixrude, L., Cohen, R E., and Singh, D.J. (1994) Iron at high pressure: linearized augmented plane wave calculations in the generalized gradient approximation. Physical Review B, 50, 6442–6445.

Stixrude, L., Cohen, R.E., and Hemley, R.J. (1998) Theory of minerals at high pressure. Reviews in Mineralogy, 37, 639–671, 1998.

Vanderbilt, D. (1990) Soft self-consistent pseudopotentials in a generalized eigenvalue formalism. Physical Review B, 41, 7892–7895.

Watanabe, H. (1982) Thermochemical properties of synthetic high-pressure compounds relevant to the earth's mantle in S. Akimoto and M. H. Manghnani, Eds., p. 441–464. High-Pressure Research in Geophysics.

Wentzcovitch, R.M., Martins, J.L., and Prize, G.D. (1993) Ab initio molecular dynamics with variable cell shape: application to $MgSiO_3$-perovskite. Physical Review Letters, 70, 3947–3950.

Wright, K. and Catlow, C.R.A. (1996) Calculation of the energetics of water dissolution in wadsleyite. Physics and Chemistry of Minerals, 23, 38–41.

Young, T.E., Green, H.W.II, Hofmeister, A.D., and Walker, D. (1993) Infrared spectroscopic investigation of hydroxyl in β-$(Mg,Fe)_2SiO_4$ and coexisting olivine: implications for mantle evolution and dynamics. Physics and Chemistry of Minerals, 19, 409–422.

Zha, C., Duffy, T.S., Mao, H. Downs, R.T., Hemley, R.J., and Weidner, D.J. (1997) Single-crystal elasticity of β-Mg_2SiO_4 to the pressure of the 410 km seismic discontinuity in the Earth's mantle. Earth and Planetary Science Letters, 147, E9 – E15.

MANUSCRIPT RECEIVED, NOVEMBER 13, 2000
MANUSCRIPT ACCEPTED, JULY 2, 2001
MANUSCRIPT HANDLED BY BJOERN WINKLER